Tefera *et al.*
Journal of Engineering and Applied Science (2023) 70:145
https://doi.org/10.1186/s44147-023-00314-5

Journal of Engineering and Applied Science

RESEARCH Open Access

Experimental investigation and optimization of cutting parameters during dry turning process of copper alloy

Aklilu Getachew Tefera[1], Devendra Kumar Sinha[1*] and Gaurav Gupta[2]

*Correspondence:
ds3621781@gmail.com

[1] Department of Mechanical Engineering, School of Mechanical, Chemical and Materials Engineering, Centre of Advanced Manufacturing Engineering, Adama Science and Technology University, Adama, Ethiopia
[2] Mechanical Engineering Department, Amity School of Engineering, Noida, India

Abstract

Increasing the quality and productivity of machined components are the main issues of machining operations in metalworking industries. The copper alloys CuZr and CuCrZr generally find applications for current-carrying structural components, seam welder wheels, shafts, and bearings flash. The manufacturing of these components is still facing challenges in the form of machining process characteristics. One of the most common machining operations for removing material is turning that produces reasonably good surface finish quality, which is influenced by different factors (speed of cut, rate of feed, tool geometry, cutting fluid, cutting tool, etc.). This research has focused on experimental study and optimization of the cutting parameters viz. cutting speed, depth of cut, and feed, for best surface finish, material removal rate, tool tip temperature as well as surface morphology during dry turning of C15000 and C18150 copper alloy using High-Speed Steel (HSS) tool The plan and design of experiment has been performed through orthogonal Taguchi L9. array. The optimum cutting settings were discovered by using the Taguchi technique and using the performance index by applying a Grey Relational Grade (GRG). The best cutting parameters for both materials were a cutting speed 1200 rpm, feed rate 0.06 mm/rev, and depth of cut 1.25 mm. The optimum factors obtained from GRA for all responses (surface roughness, MRR, and tool temperature) at the best level of cutting parameters are the same for both materials. These cutting parameters values yielded the experimental result for each response like surface roughness, MRR, and tool tip temperature (2.5 µm,12,475 mm^3/min, and 74 °C) for grade C15000 whereas (2.39 µm, 2590mm^3/min and 68 °C) for grade C18150. The optimization of cutting parameters plays a vital role in the improvement of surface finish which minimizes mechanical failures caused by wear, corrosion, and thereby increasing the productivity of the products. This investigation is expected to help all researchers working in this area of applications.

Keywords: C15000, C18150, Taguchi orthogonal array, High speed steel, Surface roughness, Metal removal rate, Tool temperature, Grey relational analysis

Introduction

The excellent mechanical, thermal, and electrical conductivities of copper and its alloys lead to them being more popular materials. Other important properties of copper and its alloys include exceptional corrosion resistance, machinability, high heat conductivity,

and excellent electrical conductivity. With extraordinarily high softening temperatures, copper zirconium is a great resistance welding material. A small addition of zirconium to copper enhances resistance to softening and resists deformation at high temperatures when normal copper would rapidly melt. Due to its excellent thermal conductivity, which minimizes sticking, it is especially helpful during the welding of galvanized materials. The two copper alloys (CuZr and CuCrZr) are more frequently used in mechanical joining techniques like rivets and screws as well as applicable in electrical applications such as switching contact bridges and separation rings [1]. Additionally, it is useful for current-carrying structural components, seam welder wheels, shafts, and bearings flash and butt-welding dies, and projection welding dies. The turning is the most widely used operation due to its advantages of high-speed removal of material and acceptable surface quality. By removing excess metal from a workpiece through the relative motion of a single-point cutting tool that is either parallel to or perpendicular to the rotating cylindrical workpiece, a workpiece is machined to the desired size and shape in the turning process [2]. The most crucial step in every turning operation is choosing the best cutting parameters to produce suitable surface quality, excessive material removal rate, and a minimum tool wear rate. The surface quality, size, and texture of the workpiece reflect the impact of the cutting parameters.

The most commonly used materials CuZr and CuCrZr find vast applications in precision components owing to their special properties like ductility, thermal conductivity, hardness, and strength. The machinability and surface characteristics of the component over its useful working life play a major role during the selection of material for machine components. To avoid the occurrence of defects such as dimensional inaccuracy, wear, corrosion, valley formation, and crack formation, there is a need to explore the machining characteristics of CuZr and CuCrZr alloys as there is a lack of sufficient investigation about machining performance and machinability data related to this material. The optimization of controllable parameters needs to be explored to achieve the best machinability and surface characteristics during the machining of CuZr and CuCrZr to make it suitable for various applications. The most important engineering problem is to maintain the optimum balance between manufacturing cost and product quality without negatively damaging the environment. The surface finish of an item is crucial in this machining process for estimating its quality [3]. Surface roughness, which has an influence on tribological characteristics, corrosion resistance, and fatigue life, is a crucial factor. It indicates the condition of tool wear and provides an indication of the quality of machined products. The type of tool, cutting parameters, tool condition (wear, built-up edge), work material machinability, vibration, etc. all have an impact on the surface [4]. Surface integrity refers to the topographical (geometric) characteristics of surfaces as well as their physical, chemical, mechanical, and metallurgical characteristics. The ongoing requirement for greater surface integrity and higher functional performance of manufactured components due to modern technological improvements in high precision and new machining capabilities has made it possible to make smaller components [5].

The function that various machining fluids, including vegetable oil, mineral oil, synthetic oil, and nanofluid-based machining fluid, play a vital role in improving MQL (minimum quantity lubrication) machinability during turning, milling, and grinding

operations. Today, minimum quantity lubrication technology is the talk of many industry sectors in terms of machining temperature, surface quality, tool wear, and tool life. It was determined that nano-particle-based machining fluid performed better than traditional machining fluid. Reduced tool wear, improved surface polish, and decreased machining oil consumption were the results of using machining fluid based on nanoparticles. Surface roughness measurements under MQL conditions were found to be lower than those under dry and wet machining environments, particularly at the greatest cutting speed [6].

Hard turning of AISI D2 steel (53 HRC) uses a multilayer coated carbide insert in a wet cutting environment and the Taguchi design of the experiment for improving the process parameters. The regression model has also been created and evaluated for suitability. The study's goal is to evaluate, using the Taguchi design of experiments how well multilayer coated carbide inserts perform during machining of hardened AISI D2 steel (53 HRC). To predict surface roughness, the experiment was created using the Taguchi L27 orthogonal array. The most effective parametric condition and S/N ratio were examined. An analysis of variance was also done to identify the key elements influencing surface roughness. According to the Taguchi S/N ratio and ANOVA, cutting speed was the second most important factor for surface roughness, while feed had the least significant effect in the studies [7].

In order to optimize, the Grey Relational technique was used to determine the ideal number of factors on multi-response characteristics. The percentage contributions of significant factors were calculated with ANOVA (surface roughness) [8]. The machining of nickel-silicon-chromium-copper (C18000) performs when it was assessed for surface roughness and peak-to-valley profile (accuracy) under optimum process parameters [9]. The goal of the study on this material was to provide a mirror finish and eliminate profile inaccuracies. Surface roughness and profile accuracy are greatly affected by the tool nose radius, feed rate, depth of cut, and spindle speed.

By determining flank wear, surface quality, and chip morphology while finishing turning AISI 52100 bearing steel (55 ± 1 HRC) in a dry environment using a carbide insert coated with various layers ($TiN/TiCN/Al_2O_3$), the researcher looks into the characteristics of machinability. ANOVA was used to analyze the effects of the machining factors, cutting speed, feed rate, and depth of cut, on the responses. Quadratic regression and an Artificial Neural Network were used to model the data. Using Taguchi-based GRA, multi-parametric optimization of cutting conditions was achieved. According to an analysis of chip morphology, a multilayer-coated carbide insert produces a lower temperature, preserves the sharpness of the cutting edge, and slows the development of tool wear [10].

The turning operations with different performance criteria were solved using a grey relational grade generated from the grey relational analysis. The Taguchi approach, which uses the grey relational grade as the performance index was able to be utilized to identify the ideal cutting parameters. The study optimizes the cutting parameters, such as cutting speed, feed rate, and depth of cut, using these features. Therefore, by using this method, complex multiple performance characteristic optimizations may be significantly optimized. It has been shown that the approach suggested by this

study improves the turning operations' performance characteristics, such as tool life, cutting force, and surface roughness, collectively [11].

Multi-objective grey analysis to define hole features in abrasive water jet drilling was carried out. To determine the pattern in which each parameter influences the process performance, the analysis of the variance of the individual responses was used. Important turning features include tool life, cutting force, and surface roughness. This strategy improved the outcomes of experiments. Therefore, by using this method, complex multiple-performance characteristic optimization can be significantly optimized. It is shown that the method recommended by this study enhances the turning operations' performance characteristics, such as tool life, cutting force, and surface roughness [12].

The L9 orthogonal array was successfully tested using the Taguchi method. Three levels of input parameters, such as cutting speed, depth of cut, and feed rate, were used in the trials, which were carried out on an all-geared lathe using carbide tools. For surface roughness, it was discovered that the feed rate was the most significant parameter, followed by the depth of cut. The reduction in surface roughness from the initial cutting settings to the optimum cutting parameters was approximately 300% and 252%, respectively [13].

The effects of temperature in tooltip on the wear of ceramic cutting insets used to machine Inconel 718 at varied hardness levels between 26 and 45 HRC. The temperature of the tooltip and the wear on the crater were examined in relation to cutting speed [14]. During the turning process, a sequence of tests was executed to monitor the temperature of the tooltip under controlled process conditions. Under dry machining circumstances, triangular cutting inserts made of silicon nitride ceramic (6190), mixed oxide ceramic (6050), and aluminum oxide ceramic (620) were employed. It was found that when cutting speed increases, cutting temperature grows monotonically. Additionally, crater wear caused by heating that builds up on the surface was close to the tooltip. In the development of temperature at the cutting tool's tip and wear, the hardness of the workpiece is a major factor, and cutting speed is second. With increased cutting speed and all cutting inserts, the temperature at the tooltip rises. All three of these ceramic inserts had an average temperature increase of 22%, for a 40% improvement in cutting speed.

The experiment's workpiece was OHNS (Oil Hardened Non-Shrinkage Steel). L9 OA was used in the studies to examine how the machining parameters affect the temperature of the tooltip [15]. The cut depth has shown the highest impact on tool tip temperature, followed by feed and spindle speed. The use of low values of depth of cut and spindle speed to achieve a minimal temperature in the case of OHNS during the work time was taken into consideration in this study. It was found that tungsten carbide tool machining produces the greatest results at medium speed and medium depth of cut, whereas polycrystalline diamond tool machining produces the best results at high speed and low depth of cut.

The experimental runs, which were carried out at cooled and ambient temperatures, were planned using the Taguchi L18. Cutting speeds, feed rates, and depth of cut were the machining parameters, and the temperature at the tool to workpiece interface was measured using a digital thermometer. Surface roughness and material removal rate were chosen as the control variables. With a 58.6% temperature drop during wet

machining and an 86.9% decrease during cool machining, the use of coolant allowed a drop in temperature between the interface of the tool and the workpiece. The major objective of this study will be a comparison of the contributions of liquid coolant to lower the cutting temperature [16]. Here, three variables speed, depth of cut, and feed rate were taken into consideration as indicators of cutting temperature and surface roughness when coolant-free and coolant-operated operations were performed with metal C45. On a CNC machine, during turning operation, the depth of cut and rotational speed were often the most significant variables affecting the cutting tool temperature and the surface in dry operation as well as in coolant operation.

In order to change a material's physical and chemical properties, heat treatment is a combination of industrial and metalworking operations. In order to give a material the desired properties, such as hardening or softening, heat treatment entails heating it to a specific temperature. The main methods for heat treatment are thermochemical treatment, surface treatment, annealing, and solution treatment. Titanium and its alloys had enhanced mechanical strength, fracture toughness, creep strength, and fatigue strength using solution treatment and age. Medical implants' surfaces can be treated to inhibit bacterial growth without affecting cell metabolism. Additionally, it improved the coefficient of friction and wear resistance of titanium alloys. The ductility, fracture toughness, thermal and dimensional stability, and creep resistance of titanium alloys were improved by annealing. The yield strength of materials was enhanced by aging [17].

The impact of the tool coating, radius of the cutting-edge, angle of chamfer, corner radius, and cutting-edge radius on the thermo-mechanical stress during cryogenic turning was investigated. The resultant surface morphology was assessed and analyzed to enhance the surface morphology, and recommendations for tool design were investigated [18].

Increasing cutting-edge radii and chamfer angles increases the subsurface qualities while decreasing the topography on the surface. Here, based on the qualities needed for the application of the manufactured component, an adjustment of the original geometry was required [19]. Examined through scanning electron microscopy (SEM), how the surface influences Abrasive Water Jet Machining (AWJM) parameters on composite material throughout the machining process. The presence of reinforcing particles contributed to the production of grooved lines, surface erosion, and ploughing materials Similarly, a high weight percentage of TiC makes the composite material tougher, which leads to poor machinability and poor surface quality. The garnet particles interact with the reinforcement particles at the same augmented weight percentage, causing the aluminum matrix to dissolve and increasing surface roughness. To achieve the required precision and concision, the surface morphology was evaluated using a novel evaluation technique that incorporates a wavelet filter and fractal theory [20].

The machining characteristics of the accelerated cooling environment (ACE) spray jet cooling technology that was used in the hard turning of D2 steel employing ceramic inserts and a minimum quantity of lubricant. It was observed that chipping and abrasion were the primary wear mechanisms. Cutting temperature and flank wear are significantly influenced by cutting speed and depth of cut, but

average surface roughness was significantly influenced by feed. At faster cutting rates and higher feeds, serrated chips were seen. The results of the investigation support the adoption of ACE in environmentally and economically challenging industrial sectors [21].

Rapid tool wear took place while cutting resulting in surface degradation and rising manufacturing costs. Chippings and distortion at the cutting edge degraded cutting tool strength and structure. Secondly, surface roughness and defects looked into the effect of tool wear on the related surface topography [22]. The mechanical characteristics like work hardening and residual stress as well as metallurgical aspects like dynamic recrystallization and grain structure, as well as surface roughness, defects (metal debris, surface cavities, smeared material, plucking, cracked carbide particles, redeposited material, feed marks, laps, and grooves) were listed [23]. Because of the enhanced non-homogeneities of the metallurgical phases inside the recast layer, micro-cracks may develop in this extremely hard, brittle layer. The main cause of cracks is thermal stress on the workpiece was brought on by large temperature swings over a short period of time as well as an unequal distribution of temperature throughout the surface area [24]. The feed mark, debris, tearing, and microvoids were the surface defects of the machined HIP workpiece. The feed mark, debris, and ripping flaws occur in the same ways as the surface of a machined forging workpiece [25].

From the literature review, it is clear that very few works have been done on C15000 and C18150 related to their behavior during dry turning operations at various boundary conditions. Also, the optimization of process parameters through GRA has been not explored much in the recent past. Therefore, in the present paper, an attempt has been made to explore the machining characteristics of widely used copper alloys C15000 and C18150. Also, optimization of controllable parameters to achieve the best machinability and surface characteristics during machining of CuZr and CuCrZr has been done.

Materials and methods

Materials and its compositions

Copper grades used in this study are C18150 and C15000, which have a high ductility but both materials have lower ductility than pure copper. The composition has been identified using a portable Optical Emission Spectrometer (OES). Table 1 below shows the composition of CuZr (C15000). Table 2 depicts the mechanical and physical properties of C15000.

Tables 3 and 4 below depict the composition of C18150 and the Mechanical and Physical properties of C18150 respectively.

Table 5 below shows the mechanical properties of HSS.

The most critical task in the turning process is to choose cutting parameters that will result in significant cutting quality and a good surface finish. Cutting parameters for C18150 and C15000 copper were selected for testing based on the knowledge available on the standard cutting parameters of copper according to tool manufacturer recommendations, manufacturer's handbook guidelines for the test sample, existing industry practice,

Table 1 Composition of CuZr (C15000) [26]

Composition	Cu	Zr	Ni	Pb	Zn	Bi
Wt%	98.94	0.565	0.0416	0.0250	0.0152	0.0250

Table 2 Mechanical and physical properties of CuZr (C15000) [26]

Properties	Metric	Imperial
Hardness (HV)	75	75
Tensile strength	415 MPa	60000psi
Poisson's ratio	0.15	0.15
Modulus of Elasticity	129GPa	18700ksi
Machinability of elasticity	20%	20%
Melting point	980°c	1796°f
Density	8.89 g/cm^3	0.321 lb/in^3

Table 3 Composition of CuCrZr (C18150) [27]

Composition	Cu	Cr	Zr	Al	Fe	Si
Wt%	98.92	1.01	0.595	0.0298	0.0567	0.0511

Table 4 Mechanical and physical properties of [27]

Properties	Metric	Imperial
Hardness (HV)	95	95
Tensile strength	379 MPa	55000 psi
Modulus of elasticity	117 GPa	17000 ksi
Poisson's ratio	0.18	0.18
Shear modulus	49.6 GPa	7200 ksi
Machinability of elasticity	20%	20%
Melting point	980 °C	1796°f
Density	8.89 g/cm^3	0.321 lb/in^3

Table 5 Mechanical properties of HSS [28]

Properties	Hardness	Young's modulus	Tensile strength	Density	Thermal expansion
Metric	750 HV	233 GPa	1280 MPa	7600 kg/m^3	12.6×10^{-6} k^{-1}

Table 6 Cutting parameters for both C15000 and C18150 [29]

Cutting parameters	Standard unit	Levels		
Cutting speed	rpm	800(N_1)	1000(N_2)	1200(N_3)
Feed rate	mm/rev	0.05(f_1)	0.055(f_2)	0.06(f_3)
Depth of cut	mm	1.05(p_1)	1.15(p_2)	1.25(p_3)

and experience. Recommended machining parameters for copper and copper alloys" continue a long tradition established by the German Copper Institute selected parameters. Table 6 below depicts the cutting parameters for both workpieces made of C15000 and C18150.

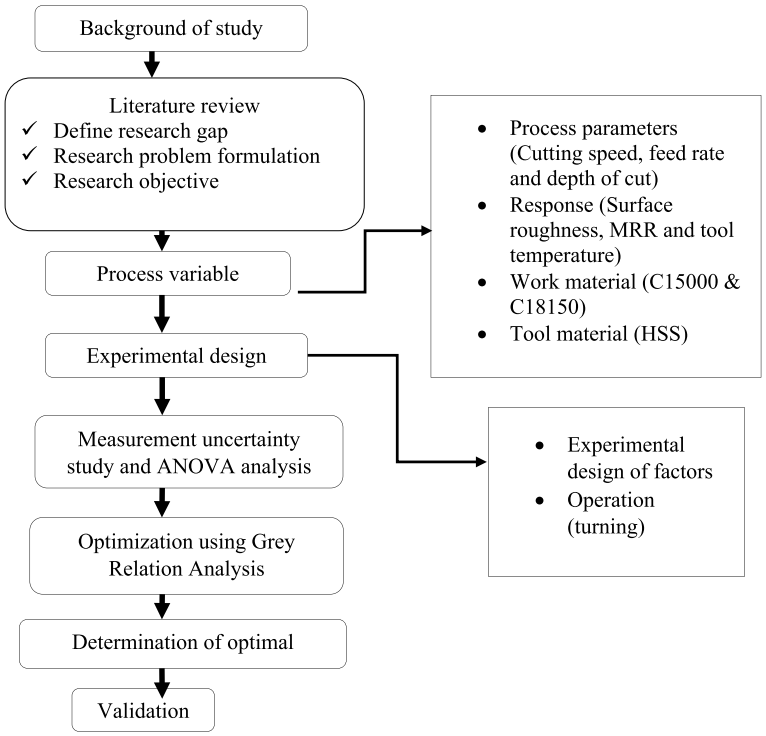

Fig. 1 Experimental procedure flow chart for determination of optimal parameters

Table 7 L9 design matrix

Exp No	Cutting parameters		
	Cutting speed (rpm)	Feed rate (mm/rev)	Depth of cut (mm)
1	800	0.050	1.05
2	800	0.055	1.15
3	800	0.060	1.25
4	1000	0.050	1.15
5	1000	0.055	1.25
6	1000	0.060	1.05
7	1200	0.050	1.25
8	1200	0.055	1.05
9	1200	0.060	1.15

Methodology

The flow chart's schematic description of the framework. The flow chart of work methodology has been depicted through Fig. 1.

Design matrix

In the present work, three factors with three levels for each have been selected and Taguchi L9 orthogonal array has been chosen.. The design matrix of variables has been shown in Table 7.

Grey relational analysis

The gray relational analysis begins by normalizing experimental data, commonly referred to as measurable aspects of the item's overall characteristics, to a range of zero to one. The correlation between the desired and actual experimental data is symbolized by the gray relational coefficient, which was determined using normalized experimental data. The total gray relational grade is then calculated by averaging the gray relational coefficients corresponding to the chosen responses [30]. The overall performance characteristic of the multiple response processes is determined by the computed gray relational grade. This strategy converts the multiple-response process optimization issue into a single-response optimization scenario because the objective function is an overall gray relational grade. The ideal parameter arrangement was subsequently selected by maximizing the total gray relational grade. Figure 2 shows the flow chart related to estimation of Grey Relational Grade.

Results and discussion

The experimentations have led to the determination of the effects of cutting parameters on surface roughness (Ra), MRR, and tool temperature during dry turning of the copper grades C15000 and C18150. These factors include the speed of the spindle, feed rate, and depth of cut. The outcomes of the experiments have been discussed in this section. In order to determine the most important cutting parameters for both materials and

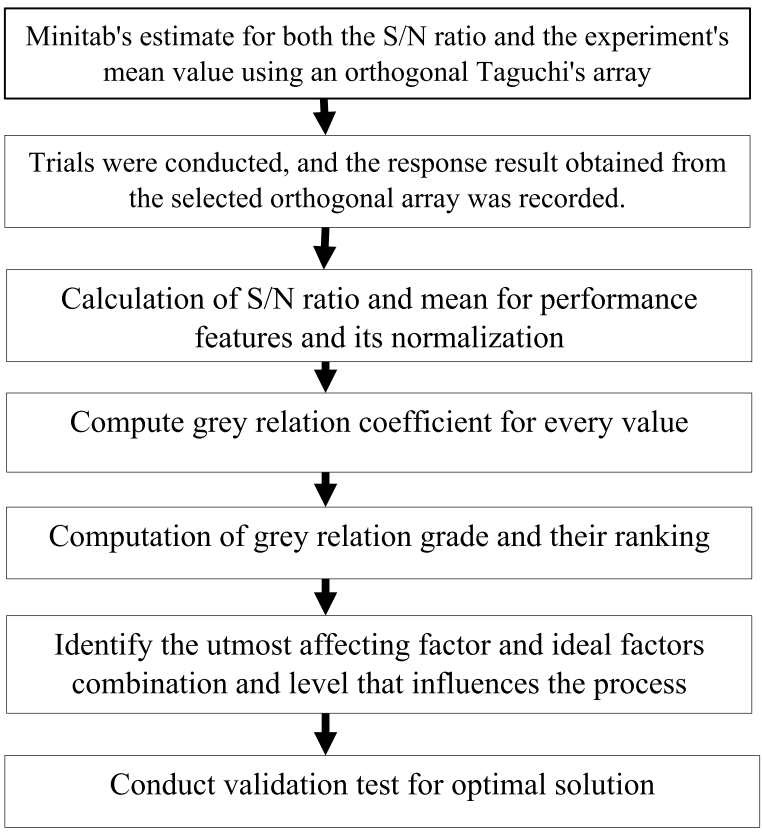

Fig. 2 Grey relational approach flowchart

determine the impact of adding chromium (Cr) to copper zirconium (CuZr), the Taguchi design was used to evaluate how cutting parameters affected response. The Grey relational technique also used to find the ideal number of variables on multi-response characteristics and to obtain the global factor.

Figure 3 demonstrates that after turning copper grades C15000 and C18150, all nine tests, each with a different combination of cutting parameters, had a cut length of 25 mm. The experimental workpiece has a 20-mm diameter. The standard copper machining feed rates are 0.05, 0.055, and 0.06 mm/rev respectively, with depth of cut of 1.25, 1.15, and 1.05 mm, cutting speed (800, 1000, and 1200 rpm), and the machining rate set at 20% for both grades of copper are the experimental conditions that were chosen for both materials. C151, C152, and C153 were made of C15000 specimens with first-level cutting speed (800 rpm), C154, C155, and C156 were made of C15000 specimens with second-level cutting speed (1000 rpm), and C157, C158, and C159 were made of specimens with third level spindle speed (1200 rpm).

Similar to the first piece with C181, C182, and C183, the second piece with C184, C185, and C186 contained C18150 specimens with second-level cutting speed(1000 rpm), and the third piece with C187, C188, and C189 contained C181500 specimens with third level spindle speed (1200 rpm) with a wide range of feed rates and depths of cut.

Surface roughness comparison for CuZr and CuCrZr

Tables 8 and 9 show the surface roughness experimental results for CuZr and CuCrZr. This demonstrates the experimental results for the levels of surface roughness (Ra) for the particular CuZr and CuCrZr turned specimens. The SN ratio for each specimen is listed in the table's final columns, and each trial value of surface roughness (Ra) in this study is the average value of two readings.

It has been observed from Fig. 4 that the surface roughness of C18150 is less as compared to C15000 at various cutting conditions. The most important characteristic common to all chromium-containing copper alloys (C18150) is that they contain sufficient chromium to make them corrosion-resistant, oxidation-resistant, and heat-resistant. As the feed rate increases at constant cutting speed, the surface roughness is increased both for CuZr and CuCrZr turned specimens. The higher feed rates signify more material in contact with the cutting tool, hence higher cutting force evolution which causes the vibration leading to high surface roughness. The increase in cutting force with an increase in feed rate may be attributed to the higher friction between the tool and the

Fig. 3 Experimental sample after turning CuZr and CuCrZr

Table 8 Experimental results of surface roughness (Ra) and S/N ratio for C15000 (CuZr)

Exp No	Cutting parameters					
	Cutting speed (rpm)	Feed rate (mm/min)	Depth of cut (mm)	I	II	Surface roughness, Average (μm)
1	800	0.050	1.05	2.63	2.67	2.65
2	800	0.055	1.15	3.38	3.36	3.37
3	800	0.060	1.25	3.43	3.39	3.41
4	1000	0.050	1.15	2.11	2.17	2.14
5	1000	0.055	1.25	2.47	2.56	2.52
6	1000	0.060	1.05	2.64	2.58	2.61
7	1200	0.050	1.25	1.97	1.91	1.94
8	1200	0.055	1.05	2.31	2.23	2.27
9	1200	0.060	1.15	1.95	1.87	2.38

Table 9 Experimental results of surface roughness (Ra) C18150 (CuCrZr)

Exp No	Cutting parameters					
	Cutting speed (rpm)	Feed rate (mm/min)	Depth cut (mm)	I	II	Average roughness of surface, (μm)
1	800	0.050	1.05	2.48	2.56	2.52
2	800	0.055	1.15	3.15	3.21	3.18
3	800	0.060	1.25	3.36	3.42	3.39
4	1000	0.050	1.15	1.96	1.98	1.97
5	1000	0.055	1.25	2.41	2.37	2.39
6	1000	0.060	1.05	2.49	2.45	2.47
7	1200	0.050	1.25	1.67	1.65	1.64
8	1200	0.055	1.05	2.13	2.05	2.09
9	1200	0.060	1.15	2.33	2.25	2.29

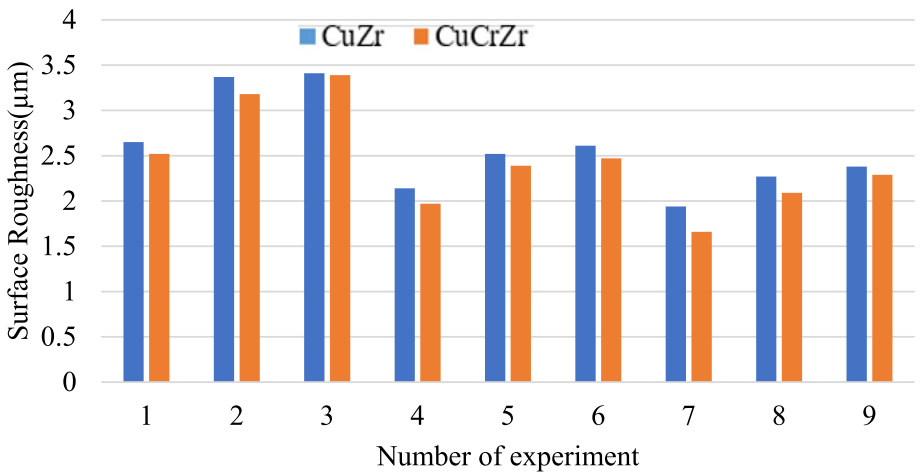

Fig. 4 Surface roughness for each experimental run

workpiece. Feed, on the other hand, negatively influences the surface roughness, where the surface finish deteriorates with an increase in feed. Higher feed rates also cause an increase in the cutting temperature, which leads to more tool wear hence undesired surface roughness. Also, the SR tends to decrease with the increase in speed with the minimum SR occurring at maximum speed. When feed increases, the SR increases. Therefore, the minimum SR prevails with the combination of maximum speed and maximum depth of cut.

The additional alloying with Cr increases the formation of the Cu oxide scale on the surface up to such a level that the Cu content in bulk can be kept within the standard limits for achieving better mechanical properties of the alloy. In most cases, heat treatment improves the strength and reduces the ductility and toughness of alloy material.

Cutting parameter effects on roughness of the surface

Feed rate influence on roughness

Figures 5, 6, and 7 demonstrate the influence of feed rate on 'Ra' at cutting speeds of 800, 1000, and 1200 rpm, respectively. The polynomial curve fitted equation shows the feed rate (x) and the average surface roughness (y). The term "coefficient of determination" refers to R^2. It determines how well the data points fit the curve. The experimental and mathematical curve fitting values are said to be in good agreement when the R^2-value is close to 1. As observed from the Figs. 5, 6, and 7, the fitted curve is approximated to R^2-value of 1.

The surface roughness of turned CuZr and CuCrZr specimens both increases as the feed rate improves at the same cutting speed, as depicted in Fig. 5. As more material comes into contact with the cutting tool at higher feed rates, cutting force evolution increases, resulting in vibration and a rougher surface. Because there is more friction between the tool and the workpiece, cutting force increases as the feed rate increases.

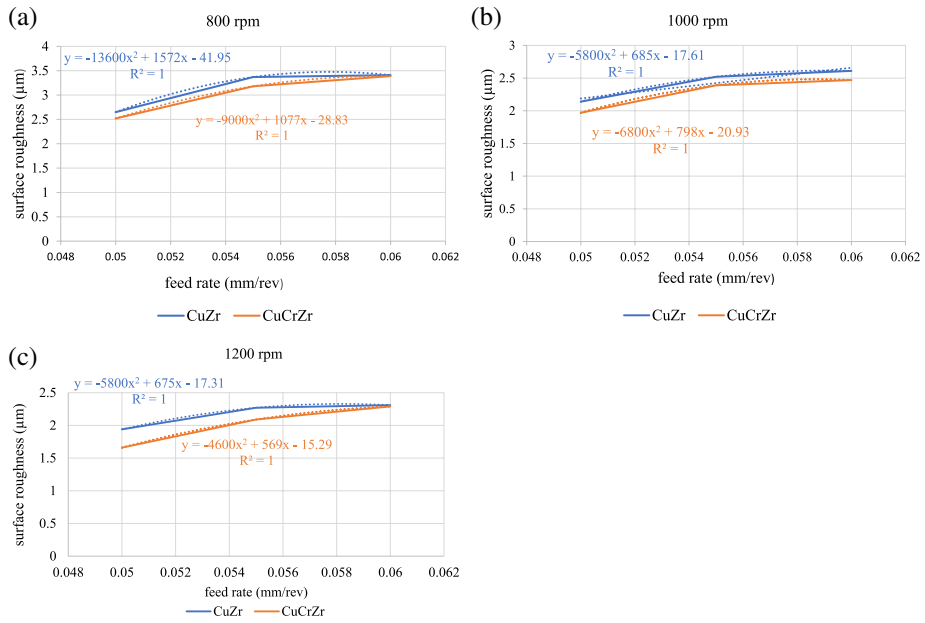

Fig. 5 Feed rate effect on surface roughness at $N = 800$, 1000, and 1200 rpm

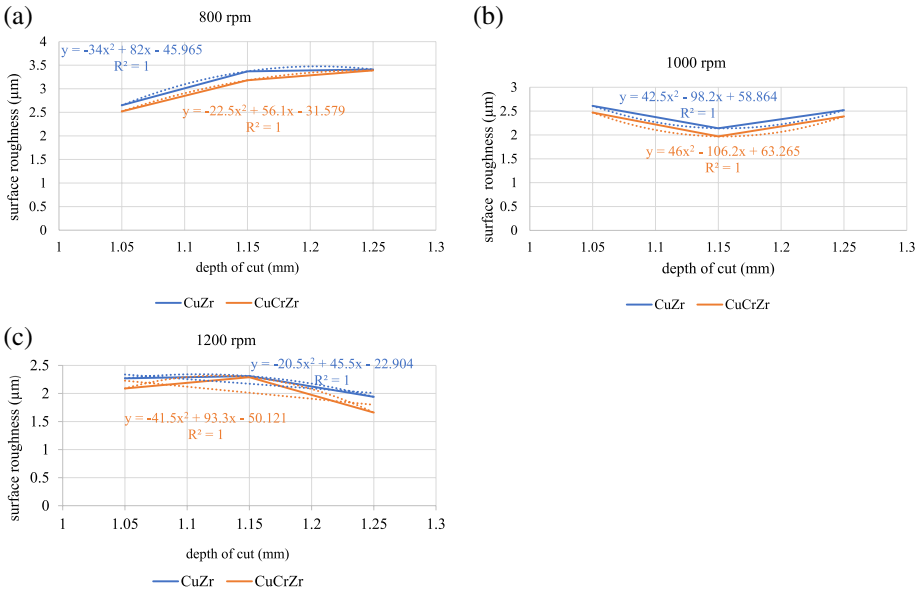

Fig. 6 Effect of depth of cut on surface roughness at $N = 800$, 1000, and 1200 rpm

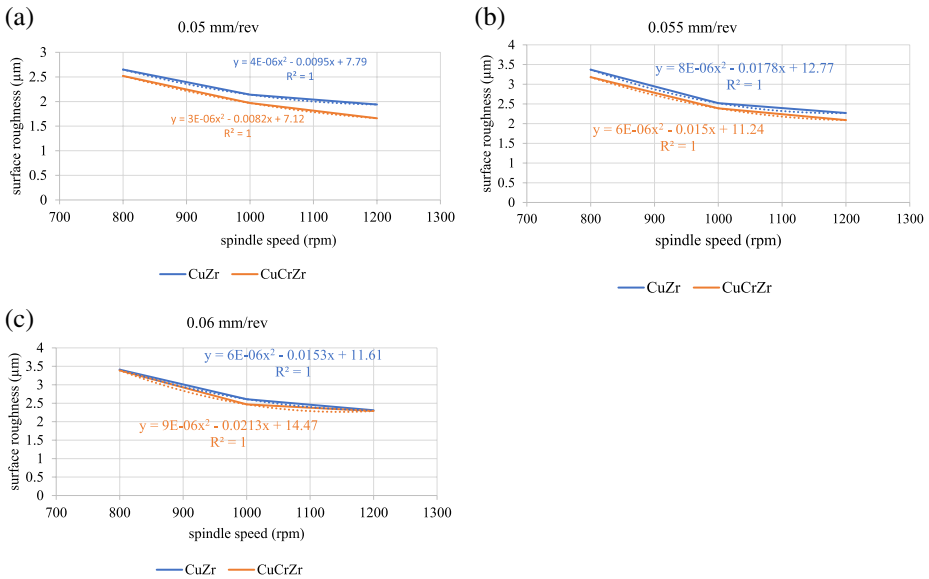

Fig. 7 Surface roughness at various feed rates at $f = 0.05$, 0.055, and 0.06 mm/rev

On the other hand, feed has a negative impact on surface roughness; as feed increases, surface finish deteriorates. Additionally, a rise in cutting temperature at higher feed rates results in increased tool wear and undesirable surface roughness. The maximum surface roughness value at a feed rate of 0.06 mm/rev and a cutting speed of 800 rpm was 3.41 µm for CuZr and 3.39 µm for CuCrZr, respectively, as cutting speed increased. When the speed of cutting was raised to 1200 rpm, it decreased to 2.29 µm for CuCrZr and 2.38 µm for CuZr, respectively.

Depth of cut effect on roughness of surface

During dry turning, the relationship between the cut depth and roughness of the surface for CuZr and CuCrZr at a constant spindle speed is depicted in Fig. 6. Surface roughness increased at constant cutting speed as the depth of cut increased because of more material removal with greater cutting forces at a deeper depth of cut.

The maximum roughness of the surface at 1.25 mm depth cut and 800 rpm cutting speed was 3.41 μm for CuZr and 3.39 μm for CuCrZr, respectively, as spindle speed increased. When the speed of the spindle was raised to 1200 rpm, it decreased to 1.94 μm for CuZr and 1.66 μm for CuCrZr, respectively. Figure 6 illustrates the influence of cut speed and depth over Ra. With increasing speed, the Ra tends to decline, with the lowest Ra occurring at the highest speed. The Ra rises as feed does in addition. With the combination of the highest speed and maximum depth of cut, the smallest Ra therefore obtained.

Effect of feed rate on surface roughness

The roughness of the turned surface decreased as the feed was increased, as can be seen.

The surface roughness was increased by spinning at a faster feed rate. CuZr and CuCrZr showed the lowest surface roughness of 1.94 m and 1.66 m, respectively, at 0.05 mm/min and 1200 rpm of feed rate.

Optimizing cutting parameters on roughness of surface (CuCrZr)

The fractional orthogonal designs of Taguchi's orthogonal arrays where the main effects are the primary focus of orthogonal array designs. Using a small number of experimental runs, these designs are used to estimate the main effects. Taguchi S/N ratios, which are log functions of the desired output, are useful as objective functions for optimization, aid in data analysis, and aid in predicting the best outcomes. The Taguchi method studies response variation using the S/N ratio.

Analysis of S/N ratios on roughness surface (CuCrZr)

By minimizing the effects of noise factors, the Taguchi design is applied to detect control factors that minimize product or process variability. Control factors are the parameters of the design and the process that can be controlled. In experimental design, the Taguchi method measures the variations in the surface roughness value using the S/N ratio. Find control factor settings that minimize the effects of the noise factors by increasing the S/N ratio. The response table for this study's SN ratios is shown in Table 10, for smaller is better.

Table 10 presents that the best combination of parameters for smaller is the better characteristic. The spindle speed is highly affected, the second one is feed rate and depth of cut have lower effects on surface roughness, which can be observed from

Table 10 S/N ratios response (CuCrZr)

Level	Cutting speed (rpm)	Feed rate (mm/rev)	Depth cut (mm)
1	− 9.560	− 6.071	− 7.428
2	− 7.104	− 8.006	− 7.712
3	− 5.966	− 8.552	− 7.490
Delta	3.595	2.480	0.283
Rank	1	2	3

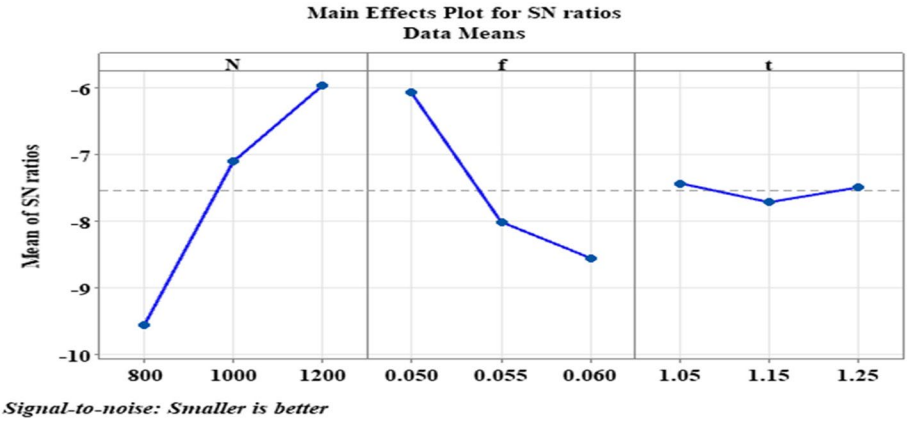

Fig. 8 Main effect plots for S/N ratio (CuCrZr)

Table 11 Optimum setting levels for parameters

Control factors	Level selected	Level value	Rank of response affected
Cutting speed	3	1200 rpm	1
Feed rate	1	0.05 mm/rev	2
Depth of cut	1	1.05 mm	3

rank table row and it is the probable combinations of parameters for enhancing the property of specimen's surface. Figure 8 shows a plot of the main effect of the control factor for the roughness of the surface S/N ratio.

The effect of a steeper slope in the S/N ratio implies that the cutting parameter has a greater impact on the surface roughness (Ra) (Fig. 8). The surface roughness is diminishing with cutting speed up from 800 to 1200 rpm. In this way, the ideal cutting velocity level is 1200 rpm. The effect of the parameter feed rate on the surface roughness values is shown above in terms of the S/N ratio. As feed increases, the surface roughness decreases. Therefore, the ideal feed rate is 0.05 mm/rev. The S/N ratio above illustrates the impact of cut depth on surface roughness values. As the depth cut increases, the surface roughness decreases. Therefore, the ideal depth cut is 1.05 mm.

Determining the optimum factor on surface roughness for CuCrZr

High cutting speed, lower feed rate, and depth cut were found to be the best parameters for determining the surface roughness value from S/N ratio analysis. The cutting speed of 1200 rpm, the feed rate of 0.05 mm/rev, and the depth of cut of 1.05 mm are the cutting parameters that correspond to these values. The optimal parameter settings for the roughness of the surface based on the results of the design of the experiment are depicted in Table 11. The roughness of the surface is predicted to have a mean value of 1.5344 μm and a S/N ratio of − 4.37892.

Table 12 Experimental results of MRR for CuZr and CuCrZr

Exp No	Cutting parameters						
	Cutting speed (rpm)	Feed rate (mm/rev)	Depth of cut (mm)	Cutting time for CuZr (min)	MRR for CuZr (mm^3/min)	Cutting time for CuCrZr (min)	MRR for CuCrZr (mm^3/min)
1	800	0.050	1.05	0.70	1147	0.67	1172
2	800	0.055	1.15	0.62	1415	0.58	1507
3	800	0.060	1.25	0.55	1729	0.53	1789
4	1000	0.050	1.15	0.52	1687	0.51	1705
5	1000	0.055	1.25	0.50	1881	0.49	1929
6	1000	0.060	1.05	0.52	1534	0.50	1611
7	1200	0.050	1.25	0.45	2113	0.44	2179
8	1200	0.055	1.05	0.40	2059	0.38	2110
9	1200	0.060	1.15	0.36	2437	0.35	2522

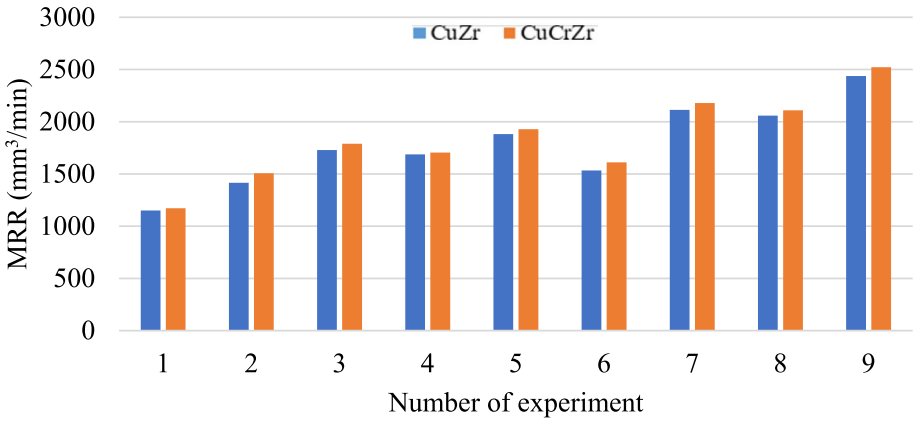

Fig. 9 Material removal rate for each experimental run

Comparison of material removal rate (MRR) for C15000 and C18150

MRR analysis

The optimal parameter combination yielded a material removal rate of 2437 and 2522 mm^3/min, as shown in Table 12. Figure 9 shows the material removal rate for every experimental run. It is observed that MRR for C18150 alloy is greater than C15000 for the defined cutting conditions.

Comparison of tool temperature for C15000 and C18150

Analysis of tool tip temperature for CuZr and CuCrZr

Heat is developed while machining any type of material due to friction, which occurs between the cutting tool and workpiece. This heat generated while machining is best if it is too low since it affects the cutting tool as well as the workpiece and disturbs the operation. The tooltip becomes softer as a result of the cutting tool's undesirable temperature, causing rapid wear on the cutting tool's materials. Many researches have contributed to ways of minimizing the temperature produced during machining. One method of minimizing this temperature is a selection of suitable cutting tools and cutting parameters for the selected workpiece. In this experimental work, the tool tip temperature generated at

Table 13 Experimental results of cutting tool temperature for CuZr and CuCrZr

Exp No	Cutting parameters				
	Spindle speed (rpm)	Feed rate (mm/rev)	Depth of cut (mm)	Temp. for CuZr (C)	Temp. for CuCrZr (C)
1	800	0.050	1.05	40.5	37.8
2	800	0.055	1.15	44.2	40.6
3	800	0.060	1.25	50.1	47.2
4	1000	0.050	1.15	52.3	50.1
5	1000	0.055	1.25	56.1	53.4
6	1000	0.060	1.05	49.5	46.7
7	1200	0.050	1.25	72.2	64.9
8	1200	0.055	1.05	62.5	58.6
9	1200	0.060	1.15	67.8	61.7

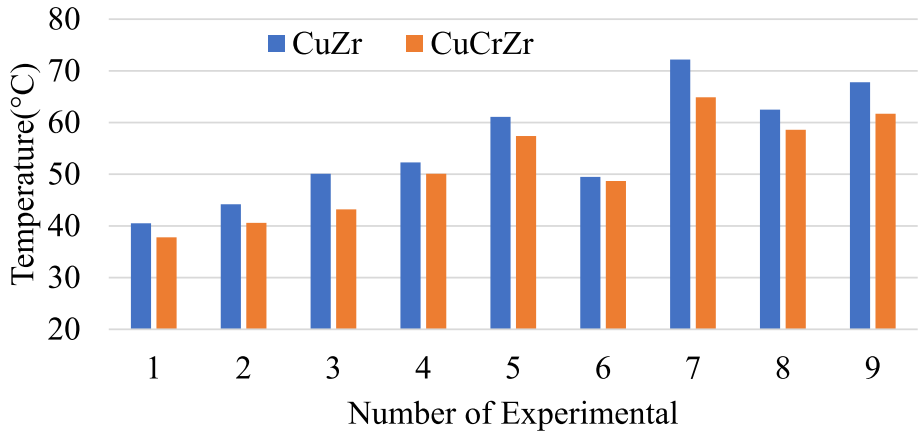

Fig. 10 Temperature for CuZr and CuCrZr on each experimental run

each run of the experiment was measured and the average temperature was acquired and displayed in Table 13. The average temperature generated during the turning of CuZr and CuCrZr varies with varying cutting parameters as shown in Table 13. As the cutting spindle speed increased, so did the cutting temperature. The morphology of the workpiece is negatively impacted by the rise in temperature. Additionally, increased heat results in dimensional changes in the machined part, making it challenging to control dimensional accuracy. It is observed from Fig. 10 that cutting tool temperature generation is higher in C15000 than in C18150 at defined cutting conditions.

Multi-objective response optimization of process parameters for CuZr and CuCrZr using TGRA

This study presents multi-objective response optimization in order to achieve the best possible surface quality, MRR, and tool temperature for both material grades. The Taguchi technique combined with Grey relational analysis was utilized to get the ideal set of three input process parameters with a focus on the quality of the machined surface, MRR, and tool temperature. Grey relational analysis may be used to evaluate even the performance of large tasks with little information. GRA is used to calculate the optimal

Table 14 Signal-to-noise ratios for CuZr on each response

Exp No	Cutting parameters			Signal to Noise ratios		
	Cutting speed (rpm)	Feed rate (mm/rev)	Depth of cut (mm)	MRR	SR	Tool Temp
1	800	0.05	1.05	− 58.181	− 8.4652	− 32.1491
2	800	0.055	1.15	66.0254	− 10.552	− 32.9084
3	800	0.06	1.25	67.7662	− 10.655	− 33.9968
4	1000	0.05	1.15	67.5526	− 6.6091	− 34.3700
5	1000	0.055	1.25	68.4981	− 8.0121	− 34.9793
6	1000	0.06	1.05	66.7268	− 8.3334	− 33.8921
7	1200	0.05	1.25	69.5083	− 5.7571	− 37.1707
8	1200	0.055	1.05	69.2834	− 7.1219	− 35.9176
9	1200	0.06	1.15	70.7474	− 5.6226	− 36.6246

Table 15 Signal-to-noise ratios for CuCrZr on each response

Exp No	Cutting parameters			Signal-to-noise ratios		
	Cutting speed (rpm)	Feed rate (mm/rev)	Depth of cut (mm)	MRR	SR	Tool Temp
1	800	0.05	1.05	− 58.3683	− 8.0291	− 31.549
2	800	0.055	1.15	66.5726	− 10.0489	− 32.170
3	800	0.06	1.25	68.0625	− 10.6043	− 33.478
4	1000	0.05	1.15	67.6448	− 5.8894	− 33.996
5	1000	0.055	1.25	68.7169	− 7.5683	− 34.550
6	1000	0.06	1.05	67.1522	− 7.8542	− 33.386
7	1200	0.05	1.25	69.7754	− 4.4023	− 36.244
8	1200	0.055	1.05	69.4959	− 6.4045	− 35.358
9	1200	0.06	1.15	71.0452	− 7.1980	− 35.805

desirable properties for a wide series of input parameters. Tables 14 and 15 show the signal-to-noise ratio of all responses to C15000 and C18150 respectively.

As part of a grey relational generation to obtain precise solutions within the range of sequences through data pre-processing, the normalization procedure is used. Data pre-processing is the process of normalizing each response between 0 and 1 in order to generate a sequence that is comparable to the original sequence. "Higher-the-better" (HB) is the form we obtained as the original sequence, then the original sequence can be normalized, and "smaller-the-better" (LB) is the form we obtained as the original sequence, then the original sequence can be normalized. Table 16 below shows the normalized value of responses. Table 17 depicts the quality loss of all responses.

Tables 18 and 19 show the grey relational coefficient which is calculated to express the relationship between the ideal and actual normalized experimental results and optimization of the complicated multiple process responses can be converted into the optimization of a single grey relational grade. The mean of the grey relational grade for each level of cutting parameters and the total mean of the grey relational grade are summarized.

The levels where the greatest normal response was attained were chosen since a larger GRG demonstrates superior diverse execution qualities. The turning operations with

Table 16 Normalized values and deviational sequences for MRR, SR, and tool temperature (CuZr)

Exp No	Normalization of S/N ratios			Quality loss (Delta)		
	MRR	SR	Tool Temp	MRR	SR	Tool Temp
1	0.0000	0.5648	0.0000	1.0000	0.4352	1.0000
2	0.9634	0.9796	0.1512	0.0366	0.0204	0.8488
3	0.9769	1.0000	0.3679	0.0231	0.0000	0.6321
4	0.9752	0.196	0.4423	0.0248	0.804	0.5577
5	0.9826	0.4748	0.5636	0.0174	0.5252	0.4364
6	0.9688	0.5386	0.3471	0.0312	0.4614	0.6529
7	0.9904	0.0267	1.0000	0.0096	0.9733	0.0000
8	0.9886	0.2979	0.7505	0.0114	0.7021	0.2495
9	1.0000	0.0000	0.8912	0.0000	1.0000	0.1088

Table 17 Normalized values and deviational sequences for MRR, SR, and tool temperature (CuCrZr)

Exp No	Normalization of S/N ratios			Quality loss (Delta)		
	MRR	SR	Tool Temp	MRR	SR	Tool Temp
1	0.0000	0.5848	0.0000	1.0000	0.4152	1.0000
2	0.9654	0.9104	0.1322	0.0346	0.0896	0.8678
3	0.9770	1.0000	0.4109	0.0230	0.0000	0.5891
4	0.9737	0.2398	0.5212	0.0263	0.7602	0.4788
5	0.9820	0.5105	0.6392	0.0180	0.4895	0.3608
6	0.9699	0.5566	0.3912	0.0301	0.4434	0.6088
7	0.9902	0.0000	1.0000	0.0098	1.0000	0.0000
8	0.9880	0.3228	0.8111	0.0120	0.6772	0.1889
9	1.0000	0.4508	0.9065	0.0000	0.5492	0.0935

Table 18 Grey relational coefficient (GRC) and grey relational grade (GRG) for CuZr

Exp No	Grey relational coefficient (GRC)			Grey relational grade (GRG)
	MRR	SR	Tool Tem	
1	0.5000	0.6968	0.5000	0.5656
2	0.9647	0.9800	0.5409	0.8285
3	0.9774	1.0000	0.6127	0.8634
4	0.9758	0.5543	0.6420	0.724
5	0.9829	0.6557	0.6962	0.7782
6	0.9698	0.6843	0.6050	0.753
7	0.9905	0.5068	1.0000	0.8324
8	0.9888	0.5875	0.8003	0.7922
9	1.0000	0.5000	0.9019	0.8006

different performance criteria were solved using a grey relational grade generated from the grey relational analysis. The optimum cutting settings were discovered by using the Taguchi technique and the grey relational grade as the performance index. The best cutting parameters for both materials: cutting speed 1200 rpm, feed rate 0.06 mm/rev, and depth cut 1.25 mm. The optimum factors obtained from GRA for all responses (surface

Table 19 Grey relational coefficient (GRC) and grey relational grade (GRG) for CuCrZr

Exp No	Grey relational coefficient (GRC)			Grey relational grade (GRG)
	MRR	SR	Tool Tem	
1	0.5000	0.7066	0.5000	0.5689
2	0.9666	0.9178	0.5354	0.8066
3	0.9775	1.0000	0.6293	0.8689
4	0.9744	0.5681	0.6762	0.7396
5	0.9823	0.6714	0.7349	0.7962
6	0.9708	0.6928	0.6216	0.7617
7	0.9903	0.5000	1.0000	0.8301
8	0.9882	0.5962	0.8411	0.8085
9	1.0000	0.6455	0.9145	0.8533

roughness, MRR, and tool temperature) at the best level of cutting parameters are the same for both the grades of material (N3 f3 p3) (Tables 20 and 21).

Confirmation of the optimum results for CuZr and CuCrZr on three responses

In this study, the confirmation experiment was conducted to verify the ideal cutting conditions. In accordance with the DOE analysis and the Taguchi approach's improvement steps, a confirmation experiment was carried out to assess the predictability of the outcome. The best parameter is used to carry out the confirmation test taking this into account. Taguchi analysis with Minitab 21 Table 22 yielded the predicted surface roughness MRR and tool temperature at optimal machining conditions.

Experimental values for three responses were also measured using these machining conditions. Both for CuZr and for CuCrZr, confirmation experiments were carried out with the GRA optimum cutting parameters derived from Taguchi analysis. The optimal level of the cutting parameter results in the same for both materials, i.e., cutting speed 1200 rpm feed rate 0.06 mm/rev and depth of cut 1.25 mm (N3 f3 p3), and the result is displayed in Table 23.

Table 20 Response signal-to-noise ratios for CuZr

Level	Cutting speed (rpm)	Feed rate (mm/rev)	Depth cut (mm)
1	− 2.620	− 3.116	− 3.146
2	− 2.483	− 1.945	− 2.124
3	− 1.849	− 1.891	− 1.682
Delta	0.770	1.226	1.463
Rank	3	2	1

Table 21 Response signal-to-noise ratios for CuCrZr

Level	Cutting speed (rpm)	Feed rate (mm/rev)	Depth cut (mm)
1	− 2.662	− 3.046	− 3.037
2	− 2.321	− 1.898	− 1.955
3	− 1.614	− 1.654	− 1.606
Delta	1.048	1.391	1.431
Rank	3	2	1

Table 22 Predicted value for responses

Material	Surface roughness (μm)	MRR (mm^3/min)	Tool temperature (°C)
C15000	2.44444	2454	72.7222
C18150	2.32111	2538	66.3222

Table 23 Result of confirmation experiments for responses

Material	Surface roughness (μm)	MRR (mm^3/min)	Tool temperature (°C)
C15000	2.51	2475	74
C18150	2.39	2590	68

Table 24 Comparison between predicted and experimental value

Material	Predicted value of Ra (μm)	Experimental value of Ra (μm)	Error %
C15000	2.44444	2.51	2.62
C18150	2.32111	2.39	2.88

Table 25 Comparison between predicted and experimental value

Material	Predicted value of MRR (mm^3/min)	Experimental value of MRR (mm^3/min)	Error %
C15000	2454	2475	0.84
C18150	2538	2590	2.007

Table 26 Comparison between predicted and experimental value

Material	Predicted value of temperature (°C)	Experimental value of Temperature (°C)	Error %
C15000	72.7222	74	1.72
C18150	66.3222	68	2.47

Tables 24, 25, and 26 show the predicted and actual response of surface roughness MRR and tool temperature using TGRA optimal cutting parameters. The relative percentage error between the fitted values predicted and the experimental values of response are computed.

The values that were predicted using the Taguchi method are pretty close to the actual value that was found through experiments. This demonstrates that responses' experimental and predicted outcomes are strongly correlated.

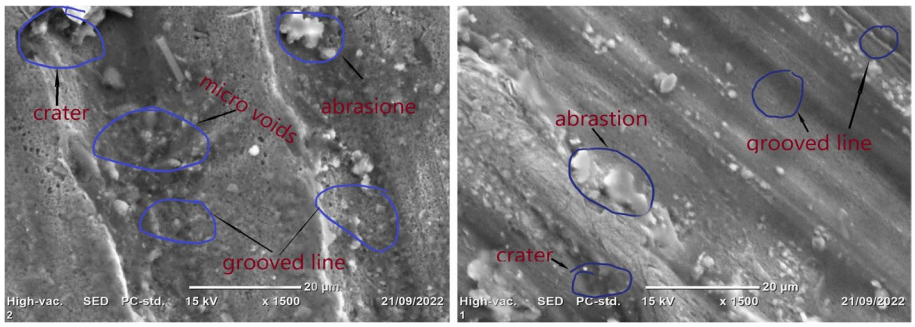

(a) (b)

Fig. 11 Surface morphology of CuZr at surface roughness value of 3.41 µm (**a**) and 1.94 µm (**b**)

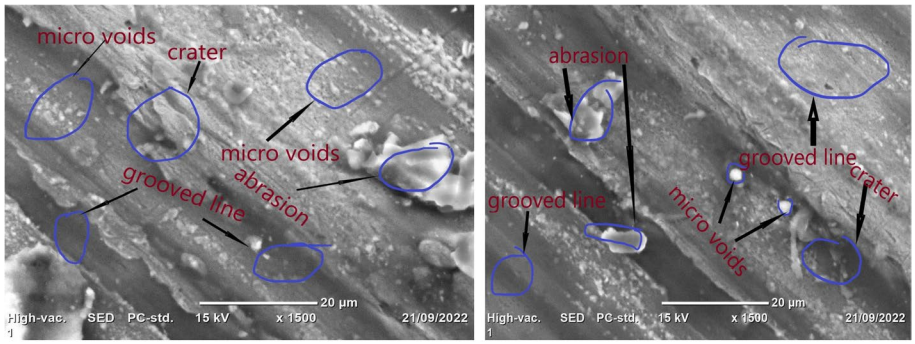

(c) (d)

Fig. 12 Surface morphology of CuCrZr at surface roughness value of 3.39 µm (**c**) and 1.66 µm (**d**)

Analysis of surface morphology defects

These surface morphological characteristics of a machined surface are behavioral indicators of defects. They include surface texture composed of roughness, waviness, and layness. Surface irregularities with a high frequency of occurring are induced by the interaction of the material microstructure and cutting tool action. The repeated form of surface defects is referred to as surface roughness. The images of the surface machined during the turning operation process are shown in Figs. 11 and 12.

The detailed microstructural investigation of the surface morphology of CuZr and CuCrZr after machining was carried out using a scanning electron microscope (SEM) and analyzed using measuring 20×20 microns and at a magnification of $\times 1500$. To obtain a good surface quality free of microvoids, abrasions, craters, grooved lines, and other surface defects, a large variety of process factors was managed during the turning process. The SEM images of the workpiece for the parameters were performed at 800 rev/min, 0.060 mm/rev, and 1.2 mm depth of cut for a higher surface roughness value, and at 1200 rev/min, 0.05 mm/rev, and 1.25 mm depth cut for a lower surface roughness value for both the grades of materials.

The SEM micrograph of the machined surface at high average roughness of surface (3.41 µm, 3.39 µm) and (1.94 µm, 1.66 µm) lower average surface roughness (Ra) value

of CuZr and CuCrZr respectively. During the machining operation, minimum particles were pulled away from the workpiece surface due to the high speed of the process, and thus microvoids and craters were formed as shown in Fig. 11b, d which was found during the casting of the material which indicates that the material does not have uniform distribution (homogeneity) of material particles.

Effect of Cr on the machining process characteristics of C15000 and C18150 during turning operation

It is observed from experimental results that spindle speed has a great effect on surface roughness and MRR on both material grades C15000 and C18150. During machining CuCrZr, it was observed that it had better deformation resistance than CuZr due to the content of chromium. In CuZr the ductility of material was reduced. The presence of chromium in CuCrZr yielded a relatively higher material removal rate in the operation as well as temperature resistance during machining which led to enhanced life of the component and tool.

The presence of Cr in C18150 strongly increases the hardenability of copper and markedly improves the resistance to corrosion and high-temperature strength or creep resistance of alloys. This reduces the defect of microstructure in CuCrZr thereby making it highly suitable in welding applications (seam welding wheel) than CuZr.

The presence of Cr in C18150 increased the deformative temperature resistance leading to less cutting tool tip generation than that in C15000.

Conclusion

This research was focused on investigating the influence of cutting parameters on the roughness of the surface, MRR, tool tip temperature, and morphology of the surface with optimization of the process parameters to get optimal end response and find the optimal global factor through GRA based approach during dry turning of C15000 and C18150 copper alloys with HSS cutting tool. The three main cutting parameters (spindle speed, depth of cut, and feed rate) with three levels for each were selected and their effects on end responses were studied. Based on the results presented in the thesis, the conclusions drawn are as follows:

1. At a depth of cut 1.25 mm, a feed rate of 0.05 mm/min, and a cutting speed of 1200 rpm, the orthogonal array yielded a minimum surface roughness of 1.94 μm for CuZr and 1.64 μm for CuCrZr.
2. Cutting speed was seen to be the important parameter for the roughness of the surface using analysis of variance (ANOVA), followed by feed rate and depth of cut having contributions of 70.20%, 29.82%, and 0.478% respectively for CuZr and 66.02%, 33.23%, and 0.434% for CuCrZr.
3. Cutting speed had the greatest impact on the material removal rate, followed by depth cut and feed rate. A higher material removal rate was observed at the highest levels of all factors for both materials were the same. The value of material removal rate at optimum cutting parameters that leads to minimum surface rough-

ness (cutting speed 1200 rpm, depth of cut 1.15 mm, and feed rate 0.06 mm/rev) was 2437 mm^3/min for CuZr and 2538 mm^3/min CuCrZr.

4. Cutting speed, followed by depth of cut and feed rate, had a significant impact on the average tool tip temperature. The temperature of the tooltip increases as the cutting speed and depth of the cut increase. At a cutting speed of 800 rpm, a depth of cut 1.05 mm, and a feed rate of 0.05 mm/rev, the lowest average temperature was achieved. CuZr and CuCrZr alloy obtained average tool tip temperatures of 40.5 °C and 37.8 °C, respectively, when cutting parameters were optimal and surface roughness was minimal.
5. The optimum cutting settings were discovered by using the Taguchi technique and the grey relational grade as the performance index. The best cutting parameters for both materials were a cutting speed of 1200 rpm, feed rate of 0.06 mm/rev, and depth of cut of 1.25 mm. The optimum factors obtained from GRA for all responses (surface roughness, MRR, and tool temperature) at the best level of cutting parameters are the same for both materials. These cutting parameters values yielded the experimental result for each response like surface roughness, MRR, and tool tip temperature (2.5 μm, 12,475 mm^3/min, and 74 °C) for grade C15000 also (2.39 μm, 2590mm^3/min, and 68 °C) for grade C18150.
6. The detailed microstructural investigation of the surface morphology of CuZr and CuCrZr after machining was carried out using a scanning electron microscope (SEM) and was analyzed at 20 × 20 microns and a magnification of × 1500. The SEM images of the workpiece were performed at 800 rev/min, 0.060 mm/rev, and 1.2 mm depth cut for a higher surface roughness value, and at 1200 rev/min, 0.05 mm/rev, and 1.25 mm depth of cut for a lower surface roughness value for both the grades of materials.
7. The SEM micrograph of the machined surface had high average roughness of surface (3.41 μm, 3.39 μm) and lower average surface roughness (Ra) of 1.94 μm and 1.66 μm for CuZr and CuCrZr respectively. When the cutting speed was lower and the feed rate and depth of cut were high, the surface had more defects like the micro void, abrasions, and crater grooves. During the machining process, the particles were pulled away from the workpiece surface due to the high speed of the process, and thus microvoids and craters were formed.

Scope for future work

The scope of future work is as follows:

1. Analysis of the effect of cutting parameters on force and tool wear rate.
2. Study the effects of tool geometry like rake angle and nose radius on the surface roughness and other process characteristics.
3. Study the effect of different cutting tools and materials with similar cutting parameters.

4. Future research work may also be directed towards applying the minimum quantity lubrication technique for further investigation of the effect of cutting parameters and to compare it with dry and wet turning.

Abbreviations

CuZr	Copper Zirconium
CuCrZr	Copper chromium zirconium
MRR	Material removal rate
S/N	Signal-to-noise ratio
ANOVA	Analysis of variance
SR	Surface roughness
SEM	Scanning electron microscope
OA	Orthogonal array
HSS	High-speed steel
GRA	Grey relational analysis

Acknowledgements
Not applicable.

Authors' contributions
Conceptualization: Akhlilu, D.K.S and G.G; methodology, Akhlilu, D.K.S and G.G; formal analysis Akhlilu, D.K.S and G.G.; investigation D.K.S.; writing—original draft preparation, and D.K.S.; writing—review and editing, D.K.S, G.G. All authors have read and agreed to the published version of the manuscript.

Funding
No funding has been given for this research work.

Availability of data and materials
The datasets used and/or analysed during the current study are available from the corresponding author on reasonable request.

Declarations

Competing interests
The authors declare that they have no competing interests.

Received: 26 July 2023 Accepted: 5 November 2023
Published online: 24 November 2023

References

1. Lai R, He D, He G, Lin J, Sun Y (2017) Study of the microstructure evolution and properties response of a friction-stir-welded copper-chromium-zirconium alloy. Metals 7(9):381
2. Rao PN (2014) Metal cutting and machine tools. Tata Mcgraw Hill Publishers 660:37–42
3. He B, Zheng H, Ding S, Yang R, Shi Z (2021) A review of digital filtering in evaluation of surface roughness. Metrol Meas Syst 28(2):217–253
4. Özen F, Fıçıcı F, Dündar M, Çolak M (2017). Effect of copper addition to aluminium alloys on surface roughness in terms of turning operation. Acta Physica Polonica a. Istanbul: Special Issue of the 6th International Congress & Exhibition (APMAS2016) 131(3):467–469.
5. Chaabani S, Arrazola PJ, Ayed Y, Madariaga A, Tidu A, Germain G (2020) Surface integrity when machining inconel 718 using conventional lubrication and carbon dioxide coolant. Procedia Manuf 47(2019):530–534
6. Roy S, Kumar R, Kumar Sahoo A, Kumar Das R (2019) A brief review on effects of conventional and nano particle based machining fluid on machining performance of minimum quantity lubrication machining. Mater Today: Proc 18:5421–5431. https://doi.org/10.1016/j.matpr.2019.07.571
7. Sahoo AK (2014) Application of Taguchi and regression analysis on surface roughness in machining hardened AISI D2 steel. International Journal of Industrial Engineering Computations, 295–304. https://doi.org/10.5267/j.ijiec.2013.11.001
8. Alagarsamy SV, Ravichandran M, Meignanamoorthy M, Chanakyan C, Kumar SD, Sakthivelu S (2020) Influence of CNC turning variables on high strength Beryllium-copper (C17200) alloy using tungsten carbide insert. Mater Today: Proc. 27:925–930
9. Taylor P, Gupta A, Ramagopal SV, Batish A, Bhattacharya A (2014) Surface roughness and profile error in precision diamond turning of C18000 surface roughness and profile error in precision diamond turning of C18000. Mater Manuf Proc 29(5):37–41.
10. Panda A, Sahoo AK, Panigrahi I, Rout AK (2018) Investigating Machinability in Hard Turning of AISI 52100 Bearing Steel Through Performance Measurement: QR, ANN and GRA Study. Int J Automoti Mech Eng 15(1):4935–4961. https://doi.org/10.15282/ijame.15.1.2018.5.0384

11. Bharat Chandra Routara, Nanda BK, Ashok Kumar Sahoo, Dhirendra Nath Thatoi, & Nayak, B. K. (2011). Optimisation of multiple performance characteristics in abrasive jet machining using grey relational analysis. 24(1/2/3/4), 4–4. https://doi.org/10.1504/ijmtm.2011.046757
12. Nair A, Kumanan S (2018) Optimization of size and form characteristics using multi-objective grey analysis in abrasive water jet drilling of Inconel 617. Journal of the Brazilian Society of Mechanical Sciences and Engineering, 40(3). https://doi.org/10.1007/s40430-018-1042-7
13. Parida AK, Das RK, Sahoo AK, Routara BC (2014) Optimization of cutting parameters for surface roughness in machining of gfrp composites with graphite/fly ash filler. Procedia Materials Science 6:1533–1538. https://doi.org/10.1016/j.mspro.2014.07.134
14. Harmain GA, Wani MF (2020) Influence of tool tip temperature on crater wear of ceramic inserts during turning process of inconel-718 at varying hardness. Tribology in Industry 42(2):310–326
15. Lata S, Rana R (2018) Investigation of chip-tool interface temperature : Effect of machining parameters and tool material on ferrous and non- ferrous metal. Materials Today: Proceedings 5(2):4250–4257
16. Abdallah F, Abdelwahab SA, Aly WI, Ahmed I (2019) Influence of cutting factors on the cutting tool temperature and surface roughness of steel C45 during turning process, Int Res J Eng Technol 6(1):1065–1072
17. Sarma J, Kumar R, Sahoo AK, Panda A (2019) Enhancement of material properties of titanium alloys through heat treatment process: a brief review. Mater Today Proc https://doi.org/10.1016/j.matpr.2019.05.409
18. Hotz H, Kirsch B (2020) Influence of tool properties on thermomechanical load and surface morphology when cryogenically turning metastable austenitic steel AISI 347. J Manuf Process 52:120–131
19. Senthilkumar TS, Muralikannan R, Kumar SS (2020) Surface morphology and parametric optimization of AWJM parameters using GRA on aluminum HMMC. Mater Today: Proc. 22:410–415
20. Feng W, Chu X, Hong Y, Deng D (2017) Surface morphology analysis using fractal theory in micro electrical discharge machining. Mater Trans 58(3):433–441
21. Kumar R, Ashok Kumar Sahoo, Purna Chandra Mishra, Rabin Kumar Das, & Manoj Ukamanal (2018) Experimental investigation on hard turning using mixed ceramic insert under accelerated cooling environment. Int J Ind Eng Comput 509–522. https://doi.org/10.5267/j.ijiec.2017.11.002
22. Liang X, Liu Z (2018) Tool wear behaviors and corresponding machined surface topography during high-speed machining of Ti-6Al-4V with fine grain tools. Tribol Int 121:321–332
23. Thakur A, Gangopadhyay S (2016) State-of-the-art in surface integrity in machining of nickel-based super alloys. Int J Mach Tools Manuf 100:25–54
24. Marashi H, Sarhan AAD, Hamdi M (2015) Employing Ti nano-powder dielectric to enhance surface characteristics in electrical discharge machining of AISI D2 steel. Appl Surf Sci 357:892–907
25. Sun FJ, Qu SG, Su F, Deng ZH, Li XQ (2018) Effect of micro-void on surface integrity after machining of Ti-6Al-4V workpieces prepared by HIP and forging. Int J Adv Manuf Technol 98(9–12):3167–3177
26. Zirconium Copper UNS C15000 (2012) AZoM.com. https://www.azom.com/article.aspx?ArticleID=6324
27. CuCrZr (C18150) C18150 Alloy. (n.d.). Alloys.copper.org. Retrieved October 12, 2023, from https://alloys.copper.org/alloy/C18150
28. Ghazali MF, Abdullah MMAB, Abd Rahim SZ, Gondro J, Pietrusiewicz P, Garus S, Stachowiak T, Sandu AV, Mohd Tahir MF, Korkmaz ME, Osman MS (2021) Tool wear and surface evaluation in drilling fly ash geopolymer using HSS, HSS-Co, and HSS-TiN cutting tools. Materials 14(7):1628. https://doi.org/10.3390/ma14071628
29. Klocke F, Lung D, Gerschwiler K, Vogtel P, Cordes S, Niehaus F (2010) Recommended machining parameters for copper and copper alloys. DKI Monograph i.18, i.18, 1–64
30. Umamaheswarrao P, Raju DR, Suman K, Sankar BR (2018) Multi objective optimization of process parameters for hard turning of AISI 52100 steel using hybrid GRA-PCA. Procedia Comput Sci 133:703–710

Publisher's Note